Genetic and pharmacological targeting of activin receptor-like kinase 1 impairs tumor growth and angiogenesis

Sara I. Cunha,[1] Evangelia Pardali,[2] Midory Thorikay,[2] Charlotte Anderberg,[1] Lukas Hawinkels,[2] Marie-José Goumans,[2] Jasbir Seehra,[3] Carl-Henrik Heldin,[4] Peter ten Dijke,[2] and Kristian Pietras[1]

[1]Department of Medical Biochemistry and Biophysics, Division of Matrix Biology, Karolinska Institutet,
 Stockholm SE-171 77, Sweden
[2]Department of Molecular Cell Biology and Centre for Biomedical Genetics, Leiden University Medical Center,
 Leiden 2300 RC, Netherlands
[3]Acceleron Pharma, Cambridge, MA 02139
[4]Ludwig Institute for Cancer Research, Uppsala University, Uppsala SE-751 05, Sweden

Members of the transforming growth factor β (TGF–β) family have been genetically linked to vascular formation during embryogenesis. However, contradictory studies about the role of TGF–β and other family members with reported vascular functions, such as bone morphogenetic protein (BMP) 9, in physiological and pathological angiogenesis make the need for mechanistic studies apparent. We demonstrate, by genetic and pharmacological means, that the TGF–β and BMP9 receptor activin receptor–like kinase (ALK) 1 represents a new therapeutic target for tumor angiogenesis. Diminution of ALK1 gene dosage or systemic treatment with the ALK1–F$_c$ fusion protein RAP–041 retarded tumor growth and progression by inhibition of angiogenesis in a transgenic mouse model of multistep tumorigenesis. Furthermore, RAP–041 significantly impaired the in vitro and in vivo angiogenic response toward vascular endothelial growth factor A and basic fibroblast growth factor. In seeking the mechanism for the observed effects, we uncovered an unexpected signaling synergy between TGF–β and BMP9, through which the combined action of the two factors augmented the endothelial cell response to angiogenic stimuli. We delineate a decisive role for signaling by TGF–β family members in tumor angiogenesis and offer mechanistic insight for the forthcoming clinical development of drugs blocking ALK1 in oncology.

CORRESPONDENCE
Peter ten Dijke:
p.ten_dijke@lumc.nl
OR
Kristian Pietras:
kristian.pietras@ki.se

Abbreviations used: ALK, activin receptor-like kinase; bFGF, basic fibroblast growth factor; BMP, bone morphogenetic protein; HUVEC, human umbilical vein endothelial cell; Id, inhibitor of differentiation; mRNA, messenger RNA; PAI, plasminogen activator inhibitor; PDGF, platelet-derived growth factor; VEGF, vascular endothelial growth factor.

The molecular mechanism for blood vessel development in tumors has been an area of intense study in recent decades. The function of prototypical angiogenic factors, such as vascular endothelial growth factor (VEGF) A, placental growth factor, basic fibroblast growth factor (bFGF), and platelet-derived growth factors (PDGFs), has been elucidated in great detail (Pietras et al., 2003; Rusnati and Presta, 2007; Ellis and Hicklin, 2008). The large knowledge base has resulted in the development of several targeted therapeutics aimed at limiting the formation of new blood vessels within tumors by neutralizing or inhibiting the action of angiogenic factors, including bevacizumab (an anti-VEGF antibody) and multireceptor tyrosine kinase inhibitors such as sunitinib, sorafenib, and imatinib (Pourgholami and Morris, 2008). However, development of new and more effective drugs aimed at targets complementary to the ones currently available for anti-angiogenic therapy is highly desirable.

The TGF–β superfamily consists of >30 secreted cytokines in mammals, including TGF–βs, bone morphogenetic proteins (BMPs), activins, and growth and differentiation factors. The family members perform diverse but important actions in embryogenesis and pathogenesis, including angiogenesis and cancer (Pardali and Moustakas, 2007; Schmierer and Hill, 2007; ten Dijke and Arthur, 2007). Cellular signaling

is initialized by ligand-induced heterotetrameric complex formation of type I and type II receptors. The prototypical ligand TGF-β_1 (hereafter referred to as TGF-β) binds to the TGF-β type II receptor (TGF-βRII), with subsequent recruitment of its type I receptors, e.g. the ubiquitously expressed activin receptor-like kinase (ALK) 5. After phosphorylation of the type I receptor by the type II receptor, downstream signaling is initiated by phosphorylation and activation of Smad transcription factors that control expression of target genes in a manner specific to type I receptor and cell-type; moreover, non-Smad pathways that modulate Smad and other major signaling pathways are initiated (Shi and Massagué, 2003; Moustakas and Heldin, 2005). In addition to intricate ligand-receptor combinations, more complexity is added by the existence of membrane-bound and soluble forms of accessory receptors, such as endoglin and betaglycan, which harbor the potential to modulate signaling specificity and intensity.

Members of the TGF-β family have been previously implicated in vasculogenic and angiogenic processes, mostly through genetic studies of mice (Seoane, 2008; Goumans et al., 2009). Germline mutations in the TGF-β type I receptor ALK1 (*ACVRL1*) or the accessory receptor endoglin (*ENG*) are causal in the development of the human syndrome hereditary hemorrhagic telangiectasia (HHT), which is characterized by telangiectases, hemorrhages, and arterio-venous malformations (Sadick et al., 2006). Although *Alk1* or *Eng* knockout mice are embryonic lethal as a result of severe vascular malformations (Arthur et al., 2000; Oh et al., 2000), mice lacking one copy of the gene for either ALK1 (*Alk1$^{+/-}$* mice) or *Eng* recapitulate the HHT phenotype with age (Srinivasan et al., 2003; Torsney et al., 2003). Despite the genetic evidence, the exact role for TGF-β signaling in angiogenesis has proved elusive. TGF-β may engage either the ubiquitously expressed type I receptor ALK5 or the predominantly vascular receptor ALK1 in endothelial cells. Although most studies find that ALK5 receptor activation inhibits endothelial cell migration, proliferation, and tube formation and that ALK1 receptor activation promotes the same processes (Goumans et al., 2002; Wu et al., 2006), there are also results indicating that endothelial cell function can be inhibited by constitutively active ALK1 receptors (Lamouille et al., 2002; David et al., 2007). Moreover, despite seemingly opposing roles on endothelial cells after stimulation with TGF-β, ALK5 receptors are obligatory for appropriate ALK1 receptor function because endothelial cells deficient for ALK5 do not induce proper TGF-β/ALK1 signaling (Goumans et al., 2003b). Furthermore, recent studies describe BMP9 and BMP10 as high-affinity ligands for ALK1 (David et al., 2007; Scharpfenecker et al., 2007). In contrast to TGF-β, signaling induced by BMP9 through ALK1 results in inhibition of both VEGF- and FGF-induced angiogenesis in vitro (David et al., 2007; Scharpfenecker et al., 2007). Finally, ALK1 is expressed mainly at sites of angiogenesis during embryogenesis (Roelen et al., 1997), but the abundance and function of ALK1 during tumor angiogenesis is largely unchartered. Clearly, there is a need for resolution of the apparent paradoxes by mechanistic

studies using well characterized in vivo models of angiogenesis and tumorigenesis.

In this paper, we demonstrate that the TGF-β family type I receptor ALK1 provides a viable new target for tumor angiogenesis. Strikingly, blunted ALK1 expression or signaling by genetic or pharmacological means delayed activation of the angiogenic switch and inhibited the growth of fully grown tumors. In seeking the molecular mechanism for the observed effects, we found an unexpected synergistic effect of TGF-β and BMP9 in stimulation of ALK1-dependent endothelial cell growth and sprouting in response to angiogenic stimuli. Our results provide mechanistic insight for the ALK1 targeting agents presently being introduced in patients and encourage the addition of molecular profiling and anti-angiogenic end points to the clinical trial designs.

RESULTS

BMP9 and TGF-β expression is increased during the tumor progression pathway of the RIP1-Tag2 model

The RIP1-Tag2 mouse model of endocrine pancreatic tumorigenesis has been widely studied (Hanahan, 1985). Because its multistep progression through a synchronous angiogenesis-dependent pathway from normal pancreatic islets to hyperplastic islets, angiogenic islets, and, finally, into overt insulinomas and because of its proven predictive value for assessing possible targets for anti-angiogenic therapies (Bergers et al., 1999), it constitutes a suitable model for investigating the role of TGF-β signaling in tumor angiogenesis. First, we determined the expression pattern of key ligands and receptors in the TGF-β signaling pathways during RIP1-Tag2 tumorigenesis. As judged by quantitative RT-PCR analysis, the expression of ALK1 was significantly increased in angiogenic islets from RIP1-Tag2 mice, as compared with other stages of normal or malignant islets (Fig. 1 a). Consistent with the reported endothelial cell–restricted expression of ALK1 (Roelen et al., 1997), other vascular markers, including CD31 and vascular endothelial cadherin, demonstrated a similar pattern of expression (Fig. S1, a and b). In contrast, the expression of ALK5 was comparatively low and remained unchanged during the tumorigenesis pathway of RIP1-Tag2 mice (Fig. 1 b). Further analysis of the βTC3 cell line established from a RIP1-Tag2 tumor (Efrat et al., 1988) revealed that tumor cells express high levels of ALK5 but not of ALK1 (Fig. S1 c). Notably, the messenger RNA (mRNA) of both TGF-β and BMP9 were present at dramatically increasing levels during the course of malignant progression in RIP1-Tag2 mice and were expressed at 5.2- and 4.4-fold higher levels in tumors compared with normal islets, respectively (Fig. 1, c and d). Expression of the ALK1 ligand BMP10 was up-regulated in angiogenic islets, albeit to a lower degree, but decreased to baseline levels in tumors (Fig. S1 d). The βTC3 cell line expressed high levels of both TGF-β and BMP9 but negligible amounts of BMP10 (Fig. S1 e). Given the structural similarity between BMP9 and BMP10, it is likely that the two ligands share many properties, so our subsequent efforts were focused on BMP9.
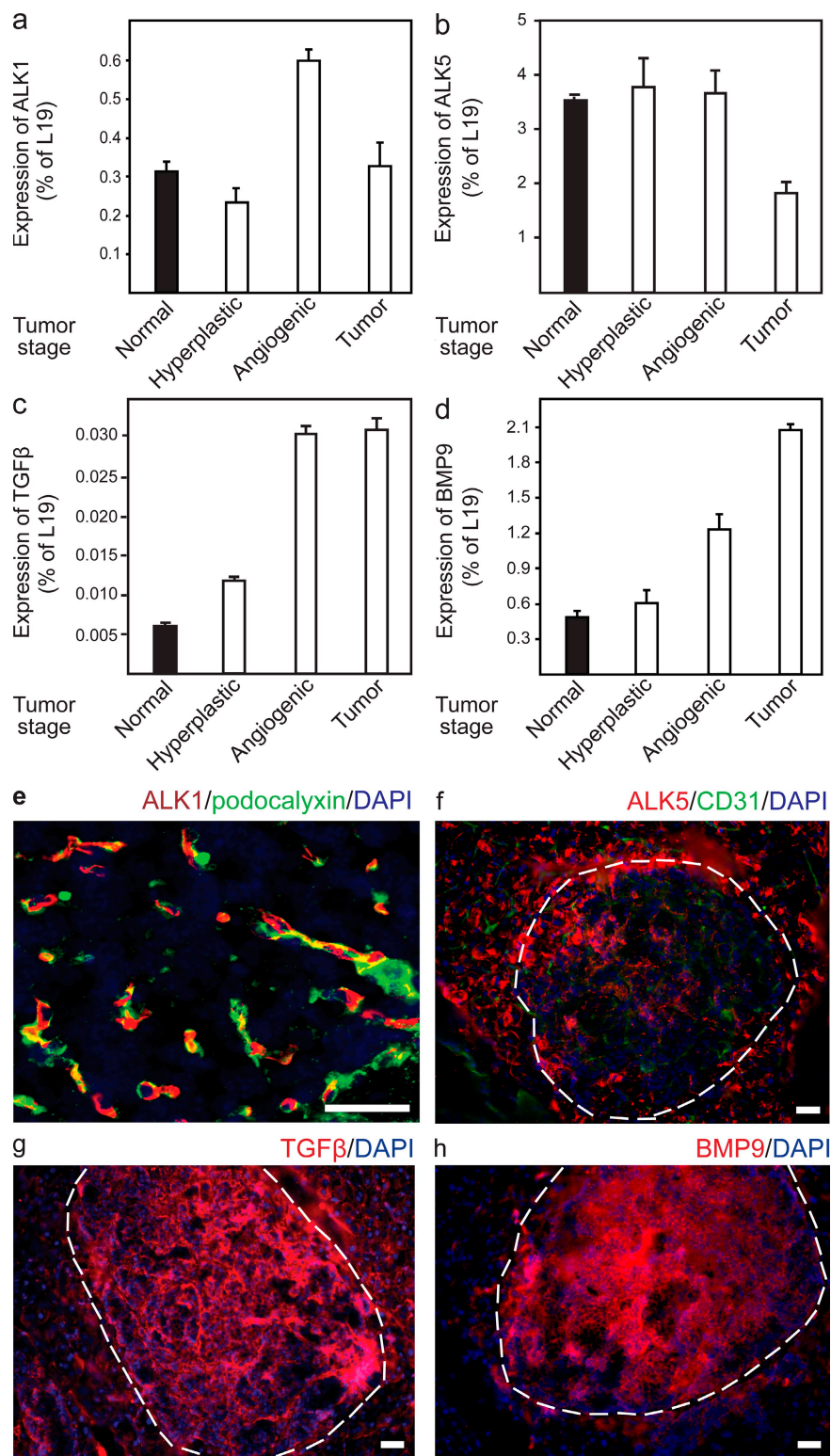
Figure 1. BMP9 and TGF-β signaling is increased during the tumor progression pathway of the RIP1–Tag2 model. (a–d) Quantitative RT-PCR analysis of the expression of ALK1 (a) and ALK5 (b) receptors and TGF-β (c) and BMP9 (d) ligands in pancreatic islets from progressive tumor stages in RIP1-Tag2 mice (materials pooled from >20 mice per tumor stage, analysis independently performed at least three times). Error bars show the mean ± SD. (e–h) Immunostaining for ALK1 (red; e), ALK5 (red; f), TGF-β (red; g), and BMP9 (red; h) of sections from the pancreas of RIP1-Tag2 mice. As a comparison, immunostaining for the endothelial cell marker podocalyxin (green) was performed in e and for CD31 (green) in f. The angiogenic islet lesional area is outlined by white dashes. Bars, 50 μm.

Next, we made use of immunostaining to ascertain which cell types expressed ALK1, ALK5, BMP9, and TGF-β in RIP1-Tag2 tumors. The specificity of the staining pattern was ascertained by omission of the primary antibody (unpublished data). As seen in Fig. 1 e, ALK1 was exclusively expressed by endothelial cells, which is in agreement with the RT-PCR analysis. The common TGF-β type I receptor ALK5 was expressed by the tumor cells of RIP1-Tag2 lesions at low levels but to a substantially higher degree by infiltrating cells in the tumor border, most likely representing inflammatory cells (Fig. 1 f). TGF-β expression was detected throughout the angiogenic and tumor lesions, most notably in the β-cells (Fig. 1 g). Finally, BMP9 was exclusively and prominently represented in the endocrine pancreas, specifically by the tumorous β-cells, and was absent from the surrounding exocrine tissue (Fig. 1 h).

Blunted ALK1 signaling retards the angiogenic switch and tumor growth in the RIP1–Tag2 model

Having documented an increased expression of TGF-β and BMP9 by malignant β cells during the tumor progression pathway of RIP1-Tag2 mice, we next sought to analyze the consequences of genetically reduced expression of their receptor ALK1. Accordingly, we crossed RIP1-Tag2 mice with mice deficient for one copy of ALK1 (RIP1-Tag2; $Alk1^{+/-}$ mice). $Alk1^{+/-}$ mice are born seemingly normal but develop vascular lesions in the skin, oral cavity, lung, liver, intestine, spleen, and brain with age (Srinivasan et al., 2003). However, no phenotype was noted in the pancreas, and the earliest time of detection for vascular abnormalities was 7 mo, i.e., a considerable time after our analysis was completed. The phenotype of RIP1-Tag2; $Alk1^{+/-}$ mice was compared with that of WT littermate RIP1-Tag2 mice (RIP1-Tag2; $Alk1^{wt}$ mice). As expected, tumors from RIP1-Tag2; $Alk1^{+/-}$ mice exhibited an ~50% reduction in the expression of ALK1, as compared with tumors from RIP1-Tag2; $Alk1^{wt}$ mice (Fig. 2 a). Interestingly, the expression of ALK5 and the accessory receptor endoglin was similarly reduced in tumors from RIP1-Tag2; $Alk1^{+/-}$ mice compared with tumors from WT mice (Fig. S2, a and b). Next, we assessed the effect of reduced ALK1 expression on the activation of the angiogenic switch by quantifying the number of angiogenic islets observed under a stereological microscope in the pancreata excised from 12-wk-old RIP1-Tag2 mice. Strikingly, RIP1-Tag2; $Alk1^{+/-}$ mice displayed a 50% reduction in the number of overtly angiogenic islets compared with RIP1-Tag2; $Alk1^{wt}$ mice (Fig. 2 b, P < 0.0001). Consistent with the reduced number of premalignant lesions, RIP1-Tag2; $Alk1^{+/-}$ mice presented with a mean of 1.55 ± 1.36 tumors per pancreas, representing a 56% reduction compared with RIP1-Tag2; $Alk1^{wt}$ mice, which developed a mean of 3.52 ± 1.78 tumors at 12 wk of age (Fig. 2 c, P < 0.001). Furthermore, the total tumor volume per mouse was significantly reduced from 42.5 ± 23.9 mm³ in RIP1-Tag2; $Alk1^{wt}$ mice to 23.1 ± 28.2 mm³ in RIP1-Tag2; $Alk1^{+/-}$ mice (Fig. 2 d, P < 0.01).

Subsequently, we sought to determine the phenotypic changes in the vascular tree as a consequence of the blunted ALK1 expression. The vascular density, as revealed by immunostaining for the endothelial cell marker CD31, was significantly lower in pancreatic lesions from RIP1-Tag2; $Alk1^{+/-}$ mice compared with RIP1-Tag2; $Alk1^{wt}$ mice (Fig. 2 e, P < 0.05). The diminished vascular tree resulted in an overall reduction in vascular perfusion of angiogenic islets and tumors by 59% in RIP1-Tag2; $Alk1^{+/-}$ mice (Fig. 2 e, P < 0.01). Collectively, we conclusively demonstrate that genetically blunted ALK1 expression retards tumor progression through the angiogenic switch, reduces de novo tumor growth, and impairs angiogenesis in the RIP1-Tag2 model of pancreatic islet carcinomas.

RAP–041 neutralizes BMP9 activity and inhibits angiogenic sprouting in vitro and in vivo

To assess whether ALK1 represents a valid therapeutic target for tumor angiogenesis, we made use of the signal transduction inhibitor RAP-041. RAP-041 is a fusion protein comprised of portions of the extracellular domain of mouse ALK1 fused to the F_c portion of IgG₁. First, we determined the neutralizing capacity and specificity of RAP-041 in vitro using luciferase reporter constructs. All ligands evaluated, including TGF-β, BMP9, and BMP10, readily activated transcription after stimulation of C2C12 cells transfected with the respective reporter constructs. BRE-luc was used for ALK1 activation and CAGA-luc was used for ALK5 activation (Dennler et al., 1998; Korchynskyi and ten Dijke, 2002; Fig. 3, a–c). RAP-041 potently suppressed the transcriptional activation induced by BMP9 and BMP10 (Fig. 3, a and b), in accordance with previous results showing that BMP9 and BMP10 are high-affinity ligands for ALK1 (David et al., 2007; Scharpfenecker et al., 2007). TGF-β–induced transcriptional activity was not neutralized by RAP-041, which is consistent with the notion that TGF-β does not bind ALK1 in the absence of TGF-βRII and ALK5 (Goumans et al., 2003b; Fig. 3 c). Consistent with these findings, RAP-041 strongly inhibited BMP9-induced Smad1 phosphorylation but not TGF-β–induced Smad2/3 phosphorylation in cell culture experiments (Fig. 3 d).

Next, we sought to analyze the inhibitory effects of RAP-041 on endothelial cell function and physiological angiogenesis. First, we seeded human umbilical vein endothelial cells (HUVECs) on Matrigel-coated plates to examine the effects of RAP-041 on endothelial cord formation. RAP-041 significantly suppressed the combined length of the resulting endothelial cell cords by 42%, as compared with control F_c protein (Fig. 3 e, P < 0.05). Also, when applied to a three-dimensional endothelial cell spheroid sprouting assay using HUVEC, RAP-041 significantly reduced VEGF-induced sprouting (Fig. 3 f, P < 0.001). Finally, RAP-041 significantly impaired the VEGF-A and/or bFGF–induced in-growth of blood vessels into subcutaneously injected Matrigel plugs in mice, compared with control F_c (Fig. 3 g, P < 0.0001; and Fig. S3, P < 0.01). We conclude that RAP-041 potently and specifically inhibits BMP9 and BMP10 activity, resulting in an impaired angiogenic response toward VEGF and bFGF.
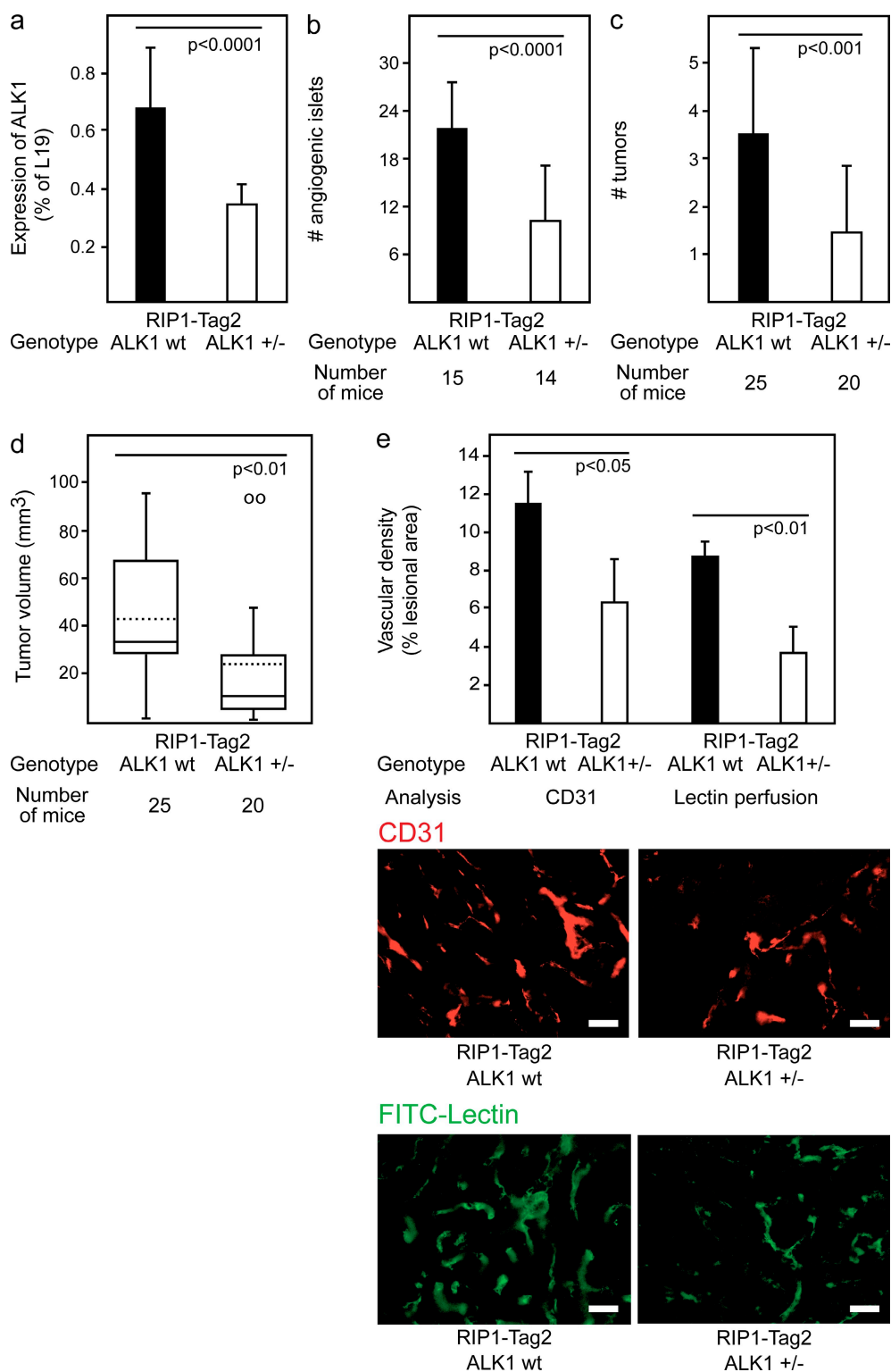
Figure 2. Blunted ALK1 signaling retards the angiogenic switch and tumor growth in the RIP1–Tag2 model. (a) Quantitative RT-PCR analysis of the expression of ALK1 in tumors from RIP1-Tag2; $Alk1^{+/-}$ mice compared with that of WT littermates (analysis independently performed at least three times). (b–d) Quantification of the number of angiogenic islets (b), the number of tumors (c), and total tumor burden (d) in RIP1-Tag2; $Alk1^{wt}$ mice and RIP1-Tag2; $Alk1^{+/-}$ mice. Box boundaries represent the interquartile range and the bars represent the full range. Solid and dotted line represents median and mean tumor volume, respectively. Circles denote statistical outliers (mean ± 2 SD). (e) Quantification of the vascular density, total (by CD31 immuno-staining), and vessels perfused (by FITC-conjugated lectin), as a percentage of the lesional area, both in RIP1-Tag2; $Alk1^{wt}$ mice and RIP1-Tag2; $Alk1^{+/-}$ mice ($n = 5$ mice for each analysis; CD31, red; FITC-lectin, green). Error bars show the mean ± SD. Bars, 50 µm.
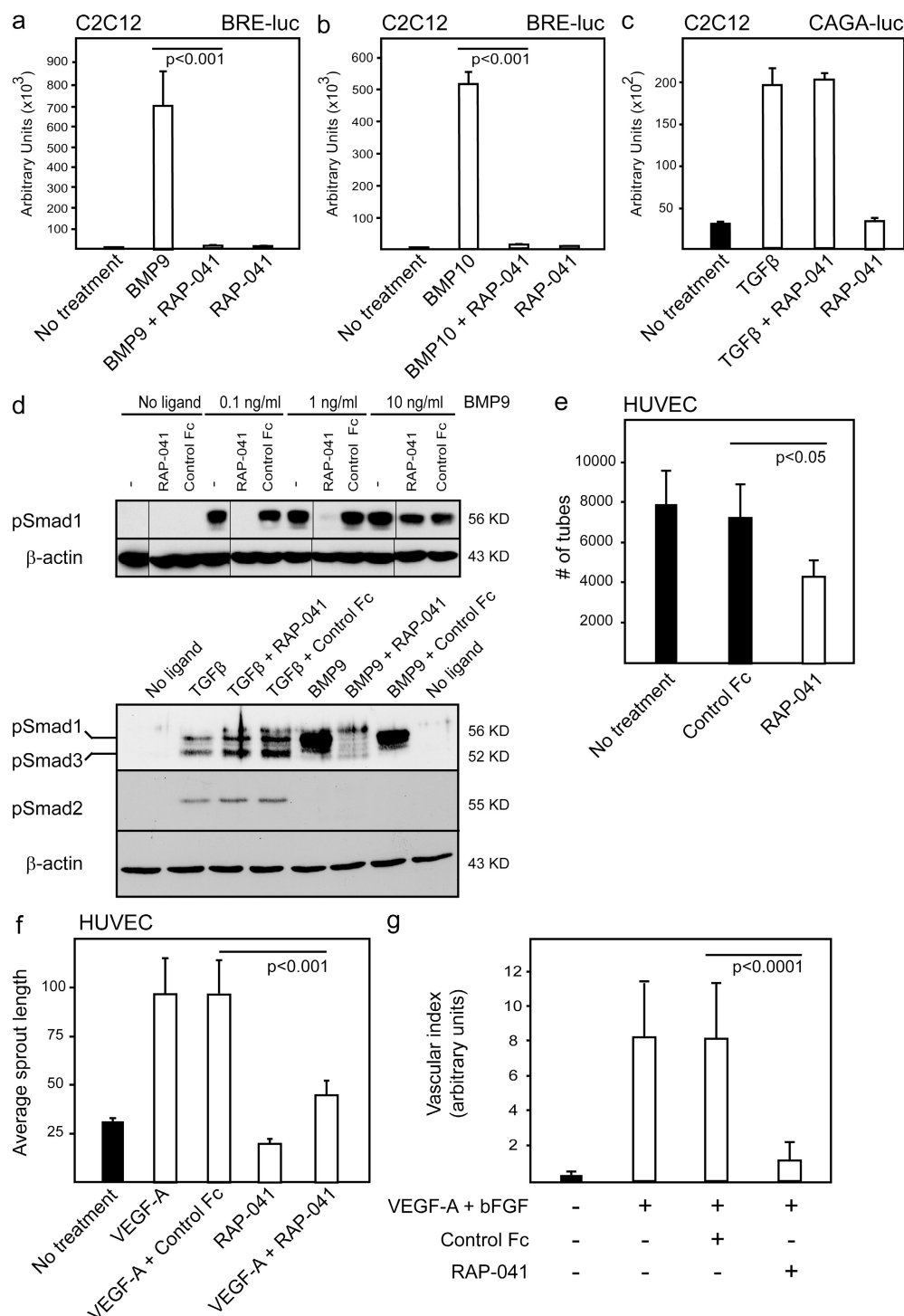
Figure 3. RAP–041 neutralizes BMP9 activity and inhibits angiogenic sprouting in vitro and in vivo. (a–c) Assessment of the capacity of RAP-041 to neutralize BMP9 (a), BMP10 (b), and TGF-β (c) by transcription activation luciferase reporter assays in C2C12 cells. Normalized promoter activity is plotted in arbitrary units as mean values from triplicate determinations (analyses independently performed at least three times). (d) Immunoblot analysis of the neutralizing activity of RAP-041 on BMP9-induced phosphorylation of Smad1 (pSmad1) in HUVEC (top) and on TGF-β–induced phosphorylation of Smad2 (pSmad2) and Smad3 (pSmad3) in C2C12 cells (bottom; analyses independently performed at least three times). The antibody used to detect pSmad3 (bottom band) also reacts with pSmad1 (top band). Immunoblotting for β-actin was used to ensure equal loading. Black lines indicate that intervening lanes have been spliced out. (e–g) Assessment of inhibition by RAP-041 of HUVEC tube formation (e) and spheroid sprouting (f; analyses independently performed at least three times) and VEGF- and FGF-induced vessels grown in subcutaneous Matrigel plugs (g; n = 5 mice per group). Error bars show the mean ± SD.

Pharmacological inhibition of ALK1 signaling retards tumor growth in the RIP1–Tag2 model

To investigate the functional consequences of pharmacological inhibition of ALK1 signaling in tumors, we treated 10-wk-old RIP1-Tag2 mice with RAP-041. Before the start of the trial, a separate cohort of RIP1-Tag2 mice was sacrificed to illustrate the initial tumor burden (Fig. 4 a). At the predefined conclusion of the trial after 2 wk of treatment, RIP1-Tag2 mice treated with 12 mg/kg control F_c protein for a total of four doses presented with a mean tumor burden of 33.3 ± 24.1 mm^3

(Fig. 4 a). Administration of an equivalent dose of RAP-041 yielded a dramatic retardation of tumor growth, with a mean tumor burden of 8.9 ± 5.3 mm^3 (Fig. 4 a, P < 0.001), which was comparable with that of the cohort sacrificed at the start of the trial (Fig. 4 a). To further characterize the efficacy of RAP-041, we performed a dose-response trial in which separate cohorts of 10-wk-old RIP1-Tag2 mice were treated with different doses of RAP-041 over the course of 2 wk. As seen in Fig. 4 b, the efficacy of RAP-041 improved with higher doses up to 12 mg/kg, after which a further increase
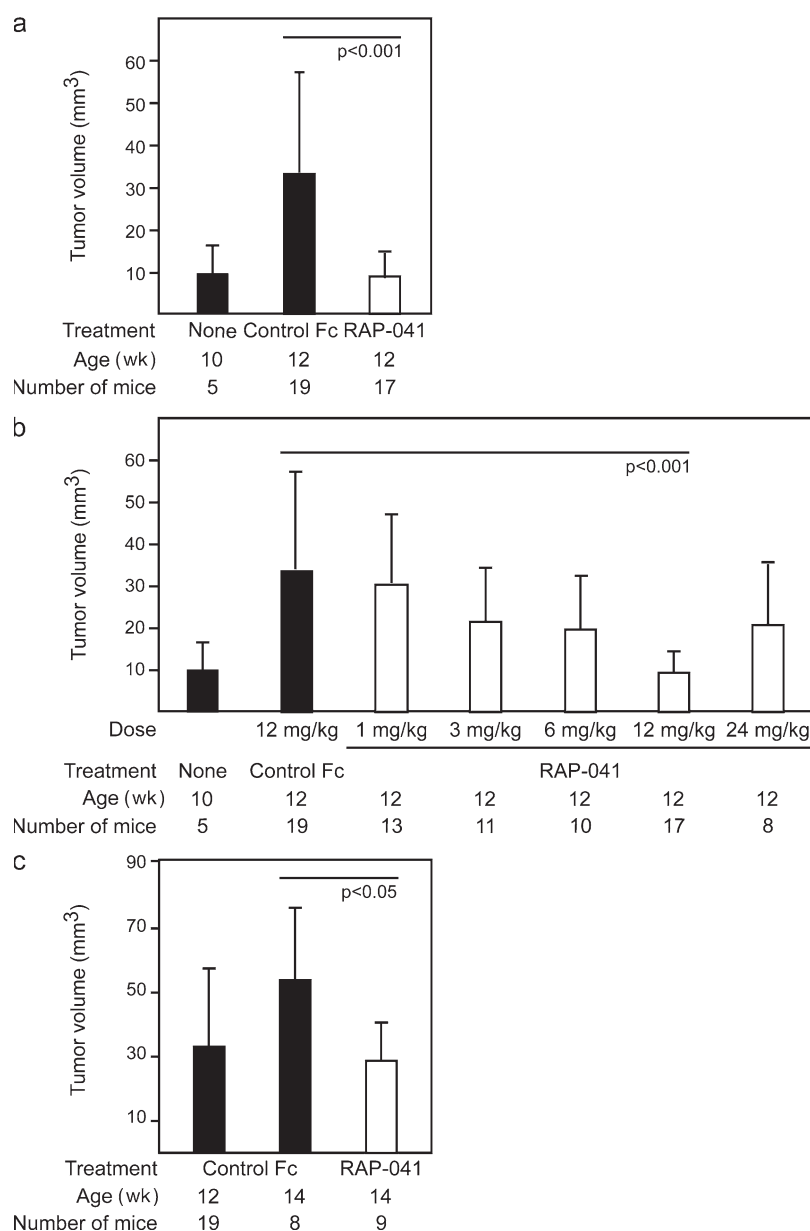
Figure 4. Pharmacological inhibition of ALK1 signaling retards tumor growth in the RIP1–Tag2 model. (a) Quantification of the total tumor burden of RIP1-Tag2 mice at 10 wk of age or after a 2-wk treatment with 12 mg/kg control F_c protein or RAP-041. (b) RAP-041 dose-response curve upon intraperitoneal injection of 1–24 mg/kg for 2 wk (10–12 wk of age). To allow a direct comparison, data for the cohort aged 10 wk, the control F_c cohort, and the 12-mg/kg cohort have been duplicated from a. (c) Quantification of the total tumor burden of RIP1-Tag2 mice at 12 wk of age or after a 2-wk treatment with 12 mg/kg of control F_c protein or RAP-041. Error bars show the mean $\pm$ SD.

to 24 mg/kg did not result in a more favorable outcome. RAP-041 was well tolerated and no overt adverse effects were observed (unpublished data).

Next, we performed a therapeutic trial at a later stage of tumor development to investigate whether RAP-041 also inhibited the growth of established bulky tumors. RIP1-Tag2 mice were treated with four injections of 12 mg/kg RAP-041 from 12–14 wk of age. In contrast to mice treated with control F_c protein, which displayed an increased mean tumor burden compared with a cohort of 12-wk-old mice, mice that received RAP-041 did not show a significant growth in their mean tumor burden during the course of the trial (Fig. 4 c; P < 0.05). We conclude that administration of the ALK1-F_c fusion protein RAP-041 dramatically retards tumor growth in RIP1-Tag2 mice, both at early and late stages of tumor development.

Treatment with RAP-041 impairs tumor angiogenesis in vivo

We characterized the effects of administration of RAP-041 on the phenotype of RIP1-Tag2 tumors. Tumors from mice treated with RAP-041, regardless of the tumor stage at the time of treatment, displayed a diminished vascular density and perfusion compared with tumors from control-treated mice (Fig. 5, a and b, vascular density, P < 0.0001 at 12 wk, P < 0.001 at 14 wk, and perfusion, P < 0.001). In addition, blood vessels in tumors from mice exposed to RAP-041 exhibited increased pericyte coverage (Fig. 5 c; P < 0.05). Although no significant difference in proliferative index was noted, the malignant β cells demonstrated a higher apoptotic index in tumors from mice treated with RAP-041, compared with tumors from control-treated mice (Fig. 5 d, P < 0.05; and not depicted). This is most likely the result of secondary effects from the anti-angiogenic phenotype because treatment of the established RIP1-Tag2 tumor cell line βTC3 with RAP-041 in vitro affected neither proliferation nor apoptosis (Fig. S4, a and b). Collectively, our findings indicate that RAP-041 inhibits tumor angiogenesis in vivo, thus limiting tumor growth by promotion of apoptosis.

Combined stimulation with TGF-β and BMP9 enhances the endothelial cell response to angiogenic stimuli

To elucidate the molecular mechanism behind the observed tumor growth inhibition by RAP-041, we performed a series of studies examining endothelial cell function in the context of an angiogenic stimulus. Importantly, both TGF-β and BMP9 were present at progressively elevated levels in RIP1-Tag2 lesions in vivo (Fig. 1 a), prompting us to investigate how the presence of both ligands affects an angiogenic response. First, we made use of three different endothelial cell lines (the MS1 mouse pancreatic islet endothelial cell line [Arbiser et al., 1997], human telomerase-immortalized microvascular endothelial cells [Venetsanakos et al., 2002], and the mouse brain endothelial cell line bEND.3) to investigate the effects of TGF-β and BMP9 signaling on endothelial cell proliferation (the mean measurement of all three cell lines is depicted in Fig. 6 a, whereas measurements for the individual cell lines are found in Fig. S5, a–c). At the chosen dose, treatment with

VEGF-A did not elicit a proliferative response of any of the endothelial cell lines (Fig. 6 a and Fig. S5, a–c). We found that the proliferation of all three cell lines was significantly retarded by either TGF-β or BMP9 alone, compared with untreated control cells (Fig. 6 a and Fig. S5, a–c). However, in sharp contrast, TGF-β together with BMP9 enhanced the mitogenic response of endothelial cells in response to VEGF-A in all cases (Fig. 6 a and Fig. S5, a–c).

Next, we investigated the effects of joint stimulation with TGF-β and BMP9 on VEGF-A and bFGF-induced angiogenesis in vivo. Matrigel plugs containing VEGF-A/bFGF with or without the supplement of TGF-β and BMP9 were injected subcutaneously into mice. Although TGF-β and BMP9 by themselves did not give rise to an angiogenic response, the addition of the two ligands significantly improved the ingrowth of blood vessels induced by VEGF-A and bFGF (Fig. 6, b and c, P < 0.001), an outcome which was effectively reverted by RAP-041 (Fig. 6, b and c, P < 0.001).

Angiogenesis in tumors from RIP1-Tag2 mice is crucially dependent on VEGF-A (Inoue et al., 2002). The effects of TGF-β and BMP9 on endothelial cell growth, as well as the observed synergy with VEGF-A in vitro and in vivo, led us to perform further experiments using a functional ex vivo model of angiogenic chemotaxis and sprouting in the RIP1-Tag2 model. We purified angiogenic islets from 12-wk-old RIP1-Tag2 mice by collagenase dissociation followed by Ficoll gradient separation. Next, the angiogenic islets were seeded into Matrigel plugs containing MS1 cells and overlaid with serum-free medium containing combinations of TGF-β, BMP9, and RAP-041. Angiogenesis-modulating factors produced by the islets will diffuse into the Matrigel and affect the phenotype and behavior of the resident endothelial cells. Under the conditions used, very little migration of endothelial cells from the angiogenic islets into the Matrigel was observed (unpublished data). When left untreated or treated with control F_c protein, the MS1 cells migrated and sprouted radially toward the angiogenic islet, demonstrating the net production of pro-angiogenic factors by the explanted tumor tissue (Fig. 6, d and e; and not depicted). Strikingly, the addition of RAP-041 to the ex vivo culture inhibited baseline migration and sprouting by 56%, indicating that BMP9 was required for efficient angiogenesis in response to the islet-produced factors, most notably VEGF-A (Fig. 6, d and e, P < 0.05). The exogenous addition of TGF-β or BMP9 alone blocked the radial in-growth of endothelial cells toward the angiogenic islet (Fig. 6, d and e, P < 0.01 and P < 0.05, respectively). In sharp contrast, the combined exogenous action of TGF-β and BMP9 negated the inhibitory effects of each ligand alone (Fig. 6, d and e, P < 0.001 vs. either factor alone and P > 0.5 vs. control). In the presence of both TGF-β and BMP9, RAP-041 again reduced the endothelial cell sprouting and migration, leaving the MS1 cells disordered on the edge of the angiogenic islet (Fig. 6, d and e, P < 0.001). Collectively, our findings demonstrate an unexpected synergy through which combined stimulation of endothelial cells with TGF-β and BMP9 negates the angiostatic effects of each ligand alone and prime endothelial cell to the pro-angiogenic
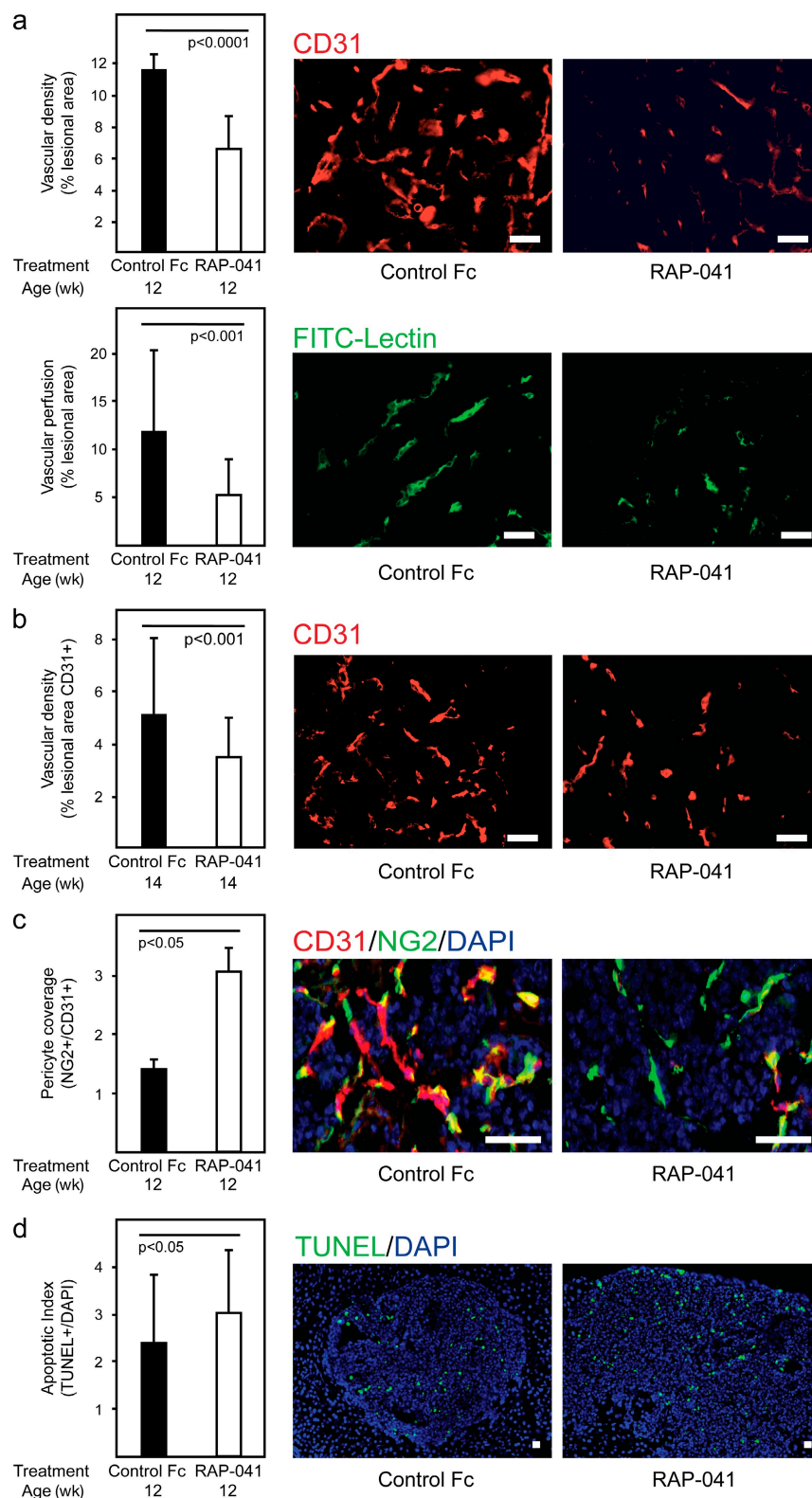
Figure 5. Treatment with RAP–041 impairs tumor angiogenesis in vivo. (a and b) Quantification of the vascular density by CD31 immunostaining (a) and by FITC-lectin perfusion (b) as a percentage of the lesional area, both in tumors from control F_c or RAP-041–treated mice of indicated age. (c) Quantification of pericyte coverage (number of NG2$^+$ cells divided by number of CD31$^+$ cells) of the vessels, as a percentage of the lesional area, of tumors from control F_c or RAP-041–treated mice. (d) Apoptotic index of tumors from control F_c or RAP-041–treated mice. $n = 5$ mice for each analysis; 10–15 high-power fields were scored for each mouse. Error bars show the mean ± SD. Bars, 50 µm.
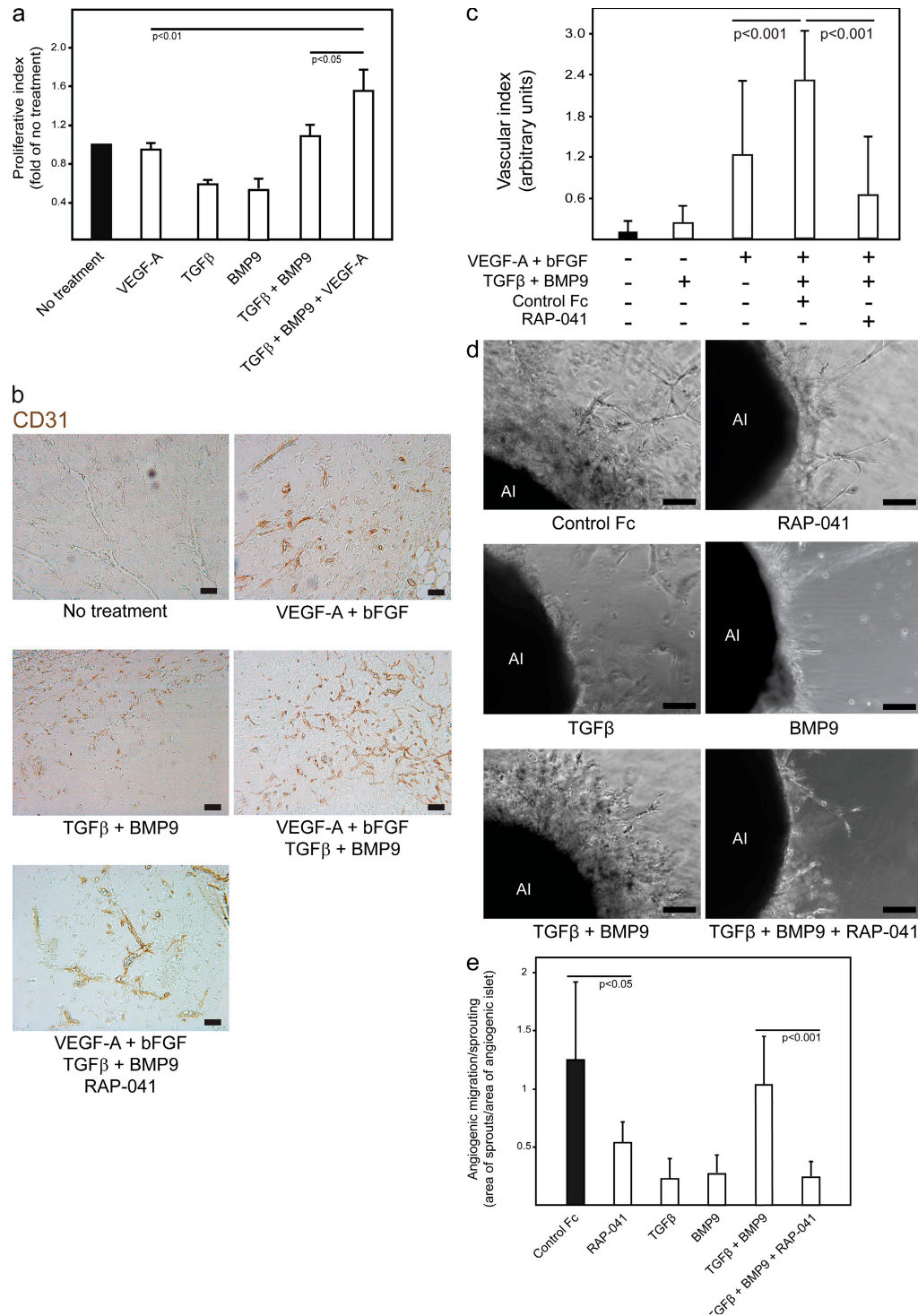
Figure 6. BMP9 and TGF–β synergistically regulate endothelial cell function. (a) Quantification of the proliferative index of endothelial cells (presented as a mean for the three endothelial cell lines MS1, bEND.3, and TIME) as a percentage of Ki67 positively stained cells over the total number of cells upon no treatment or addition of different treatments with TGF-β, BMP9, VEGF-A, and combinations thereof. (b) Immunostaining for the endothelial cell marker CD31 (brown) of subcutaneously injected Matrigel plugs containing VEGF-A + bFGF, TGF-β + BMP9, RAP-041, and combinations thereof. (c) Quantification of the vascular ingrowth, as calculated by CD31 immunostaining in subcutaneously injected Matrigel plugs containing the factors indicated. (d) Ex vivo co-culture of RIP1-Tag2 angiogenic islets and MS1 endothelial cells on Matrigel upon absence or presence of treatment with TGF-β, BMP9, RAP-041, and combinations thereof. All analyses were independently performed at least three times. (e) Quantification of the area covered by migrating/sprouting endothelial cells bordering the angiogenic islet. Each mean represents quantification of five to eight angiogenic islets per condition. Error bars show the mean ± SD. Bars, 50 μm.

action of VEGF-A and bFGF, a synergy which was effectively abrogated by RAP-041 both in vitro and in vivo.

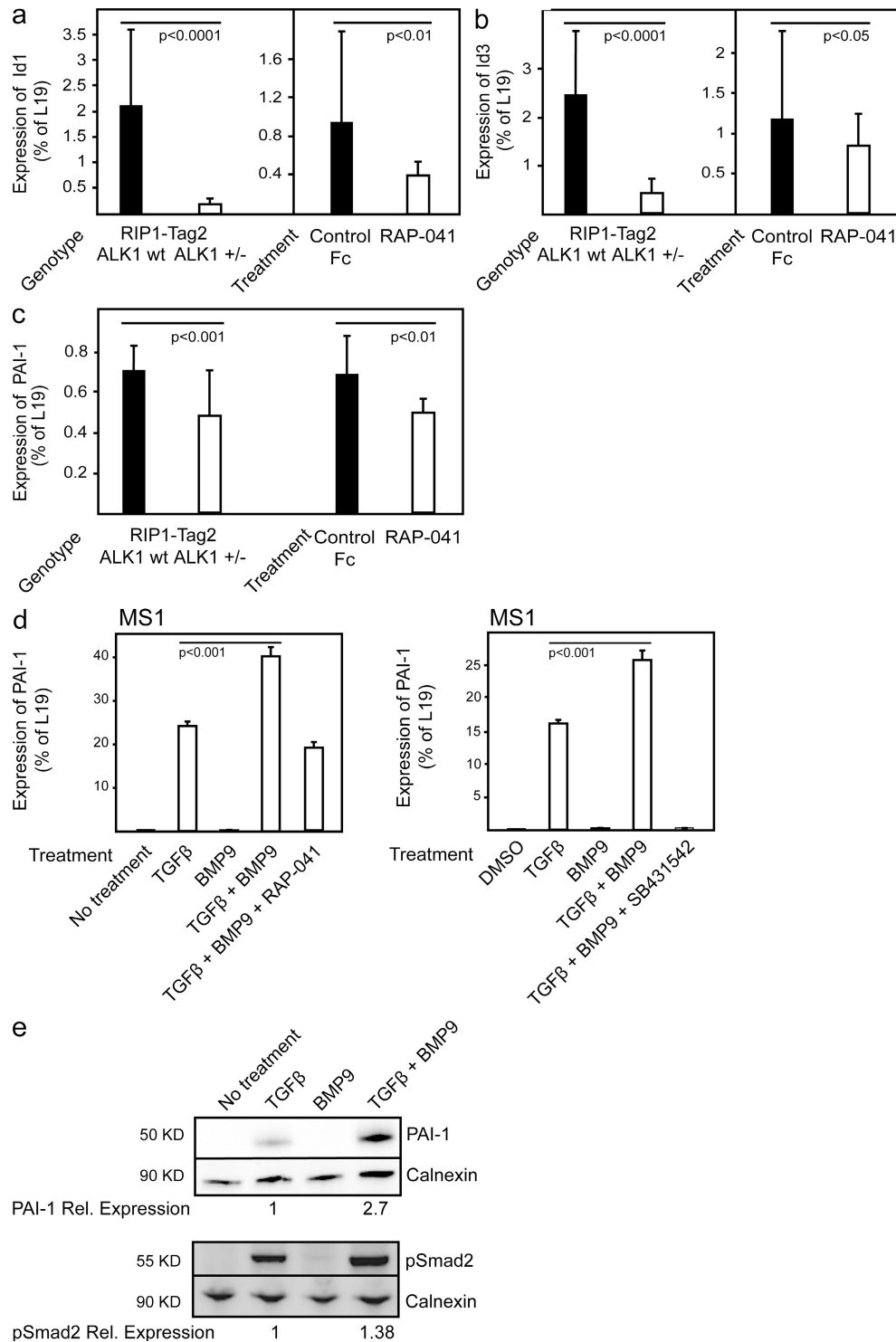## Expression of target genes for both ALK1 and ALK5 are down-regulated by blunted ALK1 signaling

To elucidate the molecular mechanism behind the observed angiogenic effects of TGF-β and BMP9 signaling, we examined the expression of known target genes with pro-angiogenic properties for ALK1 (inhibitor of differentiation [Id] 1, 2, and 3) and ALK5 (plasminogen activator inhibitor [PAI] 1, PDGF-B, and fibronectin; Goumans et al., 2002; David et al., 2007). All target genes examined were found to be dramatically up-regulated in RIP1-Tag2 angiogenic islets and/or tumors, compared with normal islets (Fig. S6, a–d; and not depicted), which is consistent with our observation that TGF-β and BMP9 were similarly induced during tumor progression. Expression analysis using mRNA from isolated endothelial cells from RIP1-Tag2 tumors revealed that Id1 was exclusively expressed by endothelial cells, whereas Id3 exhibited some expression also by other cell types (Fig. S6, e and f). Similarly, the prototypical ALK5 target genes PAI-1 and PDGF-B were predominantly expressed by endothelial cells, as ascertained by immunostaining (Fig. S6, g and h). Notably, either diminution of ALK1 gene dosage or treatment with RAP-041 gave rise to a lower expression level of Id1 and Id3 in tumors (Fig. 7, a and b). Surprisingly, tumors from RIP1-Tag2; $Alk1^{+/-}$ mice or from RIP1-Tag2 mice treated with RAP-041 exhibited reduced expression of PAI-1, indicating that ALK1 signaling affects also ALK5 target gene expression in vivo (Fig. 7 c).

We went on to appraise the transcriptional activation downstream of ALK1 and ALK5 receptors after combined ligand stimulation of cultured cells using promoter-driven luciferase constructs. Dual stimulation with TGF-β and BMP9 did not result in an increased activation of ALK1-driven transcription (Fig. S7 a). In contrast, joint signaling by TGF-β and BMP9 synergistically induced transcriptional activation of the ALK5 target gene promoter construct in transfected MS1 cells (Fig. S7 b, P < 0.01). Next, we sought to investigate whether the induction of pro-angiogenic ALK5 target genes in endothelial cells was altered after stimulation with both TGF-β and BMP9. Indeed, although TGF-β induced PAI-1 mRNA in MS1 mouse pancreatic islet endothelial cells and BMP9 had no appreciable effect, the PAI-1 mRNA was synergistically induced by combined treatment with TGF-β and BMP9 (Fig. 7 d, P < 0.001), which is consistent with the finding that TGF-β and BMP9 cooperatively activated the ALK5 target gene promoter construct. Similar results for PAI-1 were obtained using the brain endothelial cell line bEnd.3 (Fig. S7 c) and for induction of the ALK5 target gene PDGF-B in MS1 cells (Fig. S7 d, P < 0.001). Intriguingly, the synergistic induction of PAI-1 by TGF-β and BMP9 required both ALK1 and ALK5 receptors, as indicated by the use of RAP-041 and the kinase inhibitor SB431542 to selectively inhibit signaling from ALK1 and ALK5, respectively (Fig. 7 d). Western blot analysis of lysates from MS1 cells further corroborated the synergistic induction of PAI-1 expression by TGF-β and

BMP9 on the protein level (Fig. 7 e). Finally, we investigated whether the increased expression of PAI-1 was accompanied by enhanced upstream activation of TGF-β–induced signaling pathways. Indeed, combined stimulation of MS1 cells with TGF-β and BMP9 potentiated the activation of Smad2, as assessed by Western blot analysis using phospho-specific antibodies (Fig. 7 e). Thus, we have demonstrated that both ALK1 and ALK5 target genes are affected by genetically or pharmacologically diminished ALK1 signaling and that TGF-β and BMP9 synergistically induce ALK5 target genes, most likely through a Smad2-dependent pathway.

DISCUSSION

There is ample evidence from genetic studies that signaling by TGF-β family members plays an important role in angiogenesis. Deletion of either of the genes coding for TGF-β$_1$, ALK1, ALK5, TGF-βRII, Smad5, or endoglin in mice yields embryonic lethality as a result of various defects in the vascular tree (ten Dijke and Arthur, 2007). In the case of ALK1, the angiogenic defects are endothelial cell autonomous because a selective endothelial cell knockout mouse line recapitulates the global gene knockout phenotype (Park et al., 2008). In contrast, conditional knockout of the genes for ALK5 or TGF-βRII in endothelial cells did not result in overt vascular malformations (Park et al., 2008). We clearly demonstrate that $Alk1$ is a haploinsufficient gene in the context of tumor angiogenesis. RIP1-Tag2; $Alk1^{+/-}$ mice displayed a reduction in the number of angiogenic islets, as well as a reduced total tumor burden. However, there is great variation in the conclusions drawn from in vitro studies of the role of TGF-β in endothelial cell function in different contexts. As an example, low concentrations of TGF-β appear to enhance endothelial cell function in angiogenesis, whereas high concentrations of TGF-β result in opposite effects (Goumans et al., 2003a). One model to explain the apparent duality of TGF-β in endothelial cell biology is based on the fact that negative regulatory signals derived from TGF-β–induced ALK5 activation is more persistent than positive regulatory signals stemming from TGF-β–induced ALK1 activation (Goumans et al., 2003a). In this paper, we find that TGF-β by itself reduced endothelial cell proliferation and inhibited endothelial cell sprouting in an ex vivo culture of angiogenic pancreatic islets. In agreement with published results (David et al., 2007; Scharpfenecker et al., 2007), BMP9 negatively regulated endothelial cell functions to a similar degree as TGF-β. However, TGF-β and BMP9 do not act in isolation in vivo. Motivated by expression analyses demonstrating dramatically increasing levels of both TGF-β and BMP9 during the RIP1-Tag2 tumor progression pathway, we stimulated endothelial cells with both factors simultaneously. Surprisingly, the two ligands acting in concert negated the negative effects of each ligand alone and enhanced the response of endothelial cells toward VEGF-A and/or bFGF both in vitro and in vivo. These observations provide an alternative explanation for the discrepancies between different studies of TGF-β in endothelial cell function because the presence or absence of BMP9 in distinct experimental settings

Figure 7. Both ALK1 and ALK5 target gene expression is down–regulated by blunted ALK1 signaling. (a–c) Id1 (a), Id3 (b), and PAI-1 (c) mRNA expression in tumors from RIP1-Tag2; *Alk1*^{+/−} mice compared with that of WT littermates at 12 wk of age, as well as RIP1-Tag2 mice treated with control F$_c$ (Ctrl F$_c$) protein or RAP-041 between 10 and 12 wk of age. The values for each gene represent mean and SD of at least three independent experiments with three to seven tumors per experimental condition. (d) Expression of PAI-1 mRNA in MS1 endothelial cells treated with TGF-β, BMP9, RAP-041, SB431542, and combinations thereof. Error bars show the mean ± SD. (e) Western blot analysis of PAI-1 protein levels and phosphorylated Smad2 (pSmad2) levels in lysates from MS1 cells subjected to single or combined stimulation of TGF-β and BMP9. Relative expression levels were calculated by densitometric quantification of PAI-1 or pSmad2 relative to the reference protein calnexin. All analyses were independently performed at least three times.

would yield opposing results. Interestingly, TGF-β and BMP7 synergistically stimulate angiogenesis in the chick chorio-allantoic membrane assay (Ramoshebi and Ripamonti, 2000), and BMP7 potentiates TGF-β–induced activation of the E-cadherin promoter in prostate cancer cells (Buijs et al., 2007).

Blunted ALK1 signaling in the context of RIP1-Tag2 tumorigenesis gave rise to molecular changes in the expression of key regulators of angiogenesis that are characteristic for TGF-β signaling. As expected, tumors deficient for one copy of the gene encoding ALK1 exhibited diminished expression of Id1 and Id3, which is consistent with previous studies establishing these genes as specific targets of ALK1 signaling (Goumans et al., 2002). Notably, expression of Id1 and Id3 is required for tumor angiogenesis to occur (Lyden et al., 1999). Unexpectedly, the expression of the ALK5-specific target gene PAI-1 was also altered in RIP1-Tag2; $Alk1^{+/-}$ mice, giving further support to earlier studies demonstrating that ALK1 and ALK5 signaling is interdependent (Goumans et al., 2003b). Moreover, combined treatment of endothelial cells with TGF-β and BMP9 synergistically induced PAI-1, which is suggestive of a causal relationship between PAI-1 and the cooperative angiogenic effects of dual ALK1 and ALK5 activation. Even though there are results reporting cytostatic and antimigratory properties of PAI-1 in fibroblasts (Deng et al., 1996; Kortlever et al., 2006; Kortlever et al., 2008), a recent study using PAI-1–deficient mice convincingly demonstrates that tumors devoid of host-derived PAI-1 are very poorly vascularized as a result of increased endothelial cell apoptosis (Bajou et al., 2008). Together with the observed reduction of VEGF-induced angiogenesis after ALK1 inhibition, diminished expression of Id1, Id3, and PAI-1 is a likely contributing cause for the stunted angiogenic response in RIP1-Tag2; $Alk1^{+/-}$ mice. However, we do not exclude that there may be additional causal effects of blunted ALK1 expression or signaling.

Treatment of WT RIP1-Tag2 mice with optimal doses of RAP-041 yielded a near identical phenotype to that of RIP1-Tag2; $Alk1^{+/-}$ mice. Also, the molecular efficacy of RAP-041 in terms of diminishing expression of the target genes Id1, Id3, and PAI-1 appeared analogous to the genetically perturbed ALK1 pathway. Thus, because RAP-041 does not neutralize TGF-β, it is likely that BMP9 and/or BMP10 is the physiological ligand acting through ALK1 during RIP1-Tag2 tumorigenesis. Importantly, by blocking BMP9, RAP-041 reveals the anti-angiogenic effects of TGF-β without interfering with possible tumor suppressive functions that TGF-β may have in other contexts within the tumor. The therapeutic benefit from treatment with RAP-041 is comparable to that of specific inhibitors of the VEGF pathway, as observed in similar trials using the RIP1-Tag2 mouse model (Bergers et al., 2003; Pietras and Hanahan, 2005). RAP-041 inhibited VEGF-A and bFGF-induced angiogenesis in Matrigel plugs, and both TGF-β and other BMP family members, including BMP2, -4 and -6, have been demonstrated to regulate the expression of VEGF-A (Pertovaara et al., 1994; Deckers et al., 2002; Suzuki et al., 2008). Moreover, stimulation with TGF-β and BMP9 primed endothelial cells for VEGF-A and/or

bFGF-induced growth and sprouting. The exact nature of the cross talk between ALK1, ALK5 and VEGF receptor signaling pathways warrants further investigations.

Clinical benefit from targeted therapeutics aimed at the VEGF pathway has been demonstrated in several malignancies including colon, renal, lung, and breast carcinoma. Although providing a measurable prolongation of time to progression and, in some cases, also survival, most treatment regimens incorporating novel vascular targeting agents amount to a minor benefit measured in months (Hurwitz et al., 2004; Escudier et al., 2007; Motzer et al., 2007). Moreover, recent preclinical data provide evidence for the development of resistance and the emergence of more aggressive and invasive tumors after anti-angiogenic treatments (Bergers and Hanahan, 2008; Pàez-Ribes et al., 2009). It is likely that, as in the case of conventional chemotherapeutic drugs, combinations of different anti-angiogenic agents will be needed to produce long-lasting objective responses. ALK1 inhibitors are now making their appearance in clinical trials, as exemplified by ACE-041, the human counterpart of RAP-041, and PF-3446962, a humanized monoclonal antibody. Early phase clinical studies will have to determine which malignancies are most sensitive to ALK1 inhibition. Regardless of which patient group will be treated, however, our findings mandate that molecular profiling of the expression of ligands and receptors should be implemented before treatment as part of the study protocol. Our studies using both genetic and pharmacological means identify ALK1 as an attractive target for inhibiting angiogenesis in cancer. Drugs blocking ALK1 may thus be a valuable constituent in the concerted arsenal against tumor vascularization and growth.

MATERIALS AND METHODS

Quantitative RT-PCR. Total RNA was isolated using the RNeasy mini-kit (QIAGEN), after which 1 μg of total RNA served as template for RT using the iScript cDNA Synthesis kit (Bio-Rad Laboratories). Quantitative PCR was performed with an annealing temperature of 58°C on a Rotor-Gene 6000 (QIAGEN) in triplicate samples using the QuantiMix SYBR green kit (BioTools) and 1 μl of template from the RT reaction. Expression levels were calculated relative to expression of the reference ribosomal gene RPL19, as calculated by the formula $100*2^{-\Delta Ct}$. Isolated RNA from normal islets and from different stages of RIP1-Tag2 tumor progression was provided by P. Olsen and D. Hanahan (University of California, San Francisco, San Francisco, CA).

Primers used for quantitative RT-PCR. A list of the primers used for quantitative RT-PCR is shown in Table I.

Immunostaining. Cryosections were fixed with acetone. After blocking using serum-free protein block (Dako) for 90 min at room temperature (for PAI-1 staining, the Mouse-on-mouse immunodetection kit [Vector Laboratories] was used), sections were incubated overnight at 4°C with primary antibodies directed against BMP9 (ab35088; dilution, 1:500; Abcam), TGF-β (sc-146; dilution, 1:500; Santa Cruz Biotechnology, Inc.), ALK5 (AF3025; dilution, 1:25; R&D Systems), CD31 (MEC13.3; dilution, 1:100; BD), PAI-1 (Clone 41; dilution, 1:100; BD), or NG2 (AB5320; dilution, 1:400; Millipore) in PBS supplemented with 1% BSA. After three washes, sections were incubated with appropriate secondary antibodies (Invitrogen), washed, and mounted in DAPI-containing medium (Vector Laboratories).

Paraffin-embedded sections were deparaffinized followed by antigen retrieval in 0.25 mg/ml trypsin-EDTA in PBS at 37°C for 30 min. Blocking was

Table I. List of primers used for quantitative RT-PCR

Gene	5′–3′	Direction
RPL19	GGTGACCTGGATGAGAAGGA	Forward
RPL19	TTCAGCTTGTGGATGTGCTC	Reverse
ALK1	TGACCTCAAGAGTCGCAA	Forward
ALK1	CTGGGGTGCCATGTATCTTT	Reverse
ALK5	CAGAGGGCACCACCTTAAAA	Forward
ALK5	CTCGCCAAACTTCTCCAAAC	Reverse
BMP9	AACGGACAAATCGTCTACGC	Forward
BMP9	TGTGCTTCTGAAAGGGGAAG	Reverse
TGF-β	TGCTTCAGCTCCACAGAGAA	Forward
TGF-β	TGGTTGTAGAGGGCAAGGAC	Reverse
Endoglin	CACAACAGGTCTCGCAGAAA	Forward
Endoglin	GCTTGGATGCCTGAAGAGTC	Reverse
Id1	GAGTCTGAAGTCGGGACC	Forward
Id1	TTTTCCTCTTGCCTCCTGAA	Reverse
Id3	ACTCAGCTTAGCCAGGTGGA	Forward
Id3	GTCATGGGCAAAAGCTCCTC	Reverse
PAI-1	TGCATCGCCTGCCATT	Forward
PAI-1	CTTGAGATAGGACAGTGCTTTTCC	Reverse
PDGF-B	CCTCGGCCTGTGACTAGAAG	Forward
PDGF-B	CCTTGTCATGGGTGTGCTTA	Reverse
CD31	AGAGACGGTCTTGTCGCA	Forward
CD31	TACTGGGCTTCGAGAGCATT	Reverse
VE-cadherin	CAATGACAACTTCCCCGTCT	Forward
VE-cadherin	CGTTTGGGGTCTGTCTCAAT	Reverse

performed in 1% BSA and 0.5% Tween-20 in PBS. The primary antibodies against ALK1 (HPA007041; dilution, 1:100; Atlas Antibodies) and podocalyxin (AF1556; dilution, 1:100; R&D Systems) were incubated in 0.5× blocking buffer overnight at 4°C, after which appropriate secondary antibodies (1:100) were incubated in 0.5× blocking buffer for 2 h at room temperature.

Microscope image acquisition. Imaging was performed using a microscope (Eclipse E800; Nikon) equipped with Plan Fluor objectives (10×, 0.30 NA; 20×, 0.50 NA; 40×, 0.75 NA; Nikon) at room temperature in air using Alexa 594– and Alexa 488–coupled secondary antibodies. Images were acquired using a SPOT RTKE camera using the SPOT advanced software (Diagnostic Instruments, Inc.).

Animal care. All animal studies described were approved by the Stockholm north committee for animal experimentation. From 12 wk of age, all RIP1-Tag2 mice received 30% sugar water to relieve hypoglycemia. ALK1$^{+/-}$ mice were provided by S.P. Oh (University of Florida, Gainesville, FL).

Assessment of angiogenic islets and tumor incidence. Angiogenic islets were counted under a dissection microscope and defined as overtly red islets of $<1 \times 1$ mm within the pancreas. Tumors were defined as $>1 \times 1$ mm and were excised and measured with calipers. Volume was calculated using the formula $\pi/6 \times$ length $\times$ width^2.

Quantification of vascular density and perfusion. Vessel density was measured as the total number of positively stained pixels within at least eight high-power fields per mouse. Perfused functional vessels were assessed by systemic vessel labeling with FITC-conjugated tomato lectin (Vector Laboratories) injected 4 min before euthanasia.

RAP-041. RAP-041 (Acceleron Pharma) is a fusion protein comprised of aa 22–117 of the extracellular domain of mouse ALK1 fused to the F_c region

of IgG_1 and expressed in Chinese hamster ovary cells. RAP-041 was formulated in 20 mM Tris-Hcl and 0.9% NaCl. The F_c domain of IgG_1 was used as a control (IgG1 MOPC-21; Bio X Cell).

Cell culture. All cells were maintained at 37°C in a humidified atmosphere of 5% CO_2 and in medium supplemented with penicillin and streptomycin. Endothelial cells were cultured on gelatin. HUVECs were kept in Medium 199 with Earle's salt and L-glutamine (Invitrogen), 20% FBS, heparin, and bovine pituitary extract (Invitrogen). MS1, TIME, and bEND.3 cells were cultured in an Endothelial Cell Basal Medium MV2 kit (Invitrogen). βTC3 and C2C12 cells were maintained in MEM and DME, respectively, (Invitrogen) supplemented with 10% FBS and L-glutamine.

Luciferase reporter assay. C2C12 or MS1 cells were transfected using Lipofectamine LTX (Invitrogen) with 0.2 µg pGL3(BRE)-luc (Korchynskyi and ten Dijke, 2002) or pGL3(CAGA)$_{12}$-luc (Dennler et al., 1998) and 0.2 µg β-gal construct to act as internal transfection control. After 24 h, cells were treated with 10 ng/ml TGF-β, 10 ng/ml BMP9, or 50 ng/ml BMP10 in the presence or absence of 1 µg/ml RAP-041. Luciferase activity was determined after 24 h of stimulation.

Western blot analysis. For determination of RAP-041 specificity, HUVEC or C2C12 cells were starved for 5 or 24 h in medium with 1% FBS and stimulated with BMP9 or TGF-β for 45 min, washed with PBS, and lysed. For assessment of phospho-Smad2 or PAI-1 levels, MS1 cells were starved overnight in medium containing 0.1% BSA and stimulated for 30 min and 48 h, respectively. Protein concentration was quantified by DC protein assay (Bio-Rad Laboratories) and lysates were subjected to SDS-PAGE and Western blotting. Smad phosphorylation was detected with antiserum specifically recognizing phosphorylated Smad1/5 (Persson et al., 1998) or Smad2 (Piek et al., 1999), PAI-1 was detected using antibody ab28207 (Abcam), and calnexin levels were determined using sc-6465 (Santa Cruz Biotechnology, Inc.). Relative expression level was determined by densitometric quantification of PAI-1 or phosphorylated Smad2 corrected for the levels of calnexin for that particular lane.

HUVEC cord formation. Matrigel basement membrane matrix, growth factor reduced (BD), was added to a 96-well plate and allowed to polymerize for 1 h at 37°C. HUVECs (3×10^3 cells/well) were resuspended in Medium 199 containing 4% FBS and 10 µg/ml RAP-041, 10 µg/ml control F_c, or vehicle control and seeded in triplicates. Plates were incubated for 16 h. Pictures were acquired with a phase-contrast microscope in four different fields. The length of branches was quantified using automated image analysis using Analysis software (Olympus).

HUVEC spheroid sprouting assay. The endothelial sprouting assay was performed as described previously (Hawinkels et al., 2008). Spheroids (750 cells/well) were prepared by culturing HUVEC in complete medium containing 0.1% methylcellulose. The next day spheroids were collected and embedded in a collagen type 1 matrix and incubated with 50 ng/ml recombinant human VEGF (R&D Systems) with addition of control F_c protein or RAP-041.

Matrigel plugs. Male 7–8-wk-old C57BL/6 mice (Charles River Laboratories) were injected subcutaneously near their abdominal midline with 0.3 ml of Matrigel basement membrane at a high concentration (BD) combined with PBS, 2 ng/ml TGF-β, 2 ng/ml BMP9, or 300 ng/ml VEGF and 700 ng/ml bFGF-2 in the presence or absence of 20 µg/ml RAP-041 or 20 µg/ml of control F_c protein. Groups of four plugs were injected for each treatment and the experiment was repeated twice. 7 d later, Matrigel plugs were removed, fixed in formalin, and embedded in paraffin. Sections were deparaffinized. Quenching of endogenous peroxidase activity was done using 0.3% H_2O_2 in methanol for 20 min at room temperature, followed by antigen retrieval using citrate buffer and blocking with 1% BSA in PBS for 1 h at room temperature. The primary antibody against CD31 (1:1,000; Santa Cruz Biotechnology, Inc.) was incubated in 1% BSA in PBS overnight at room temperature. Biotinylated conjugated secondary antibodies were applied, followed by amplification using the strep-AB-complex/HRP (Dako).

Finally, diaminobenzidine substrate (Sigma–Aldrich) was added to visualize peroxidase activity. The area covered by CD31-positive staining was quantified with image analysis.

Therapeutic trials. RIP1-Tag2 mice were treated with control F_c or RAP-041 at indicated doses diluted in Tris–buffered saline. Treatment was given twice weekly for 2 wk by intraperitoneal injection.

Assessment of apoptosis. Apoptosis was visualized using the In situ Cell Death Detection kit (Roche). The apoptotic index was expressed as percentage of positive cells, and was assessed in 10–15 high-power fields per mouse.

In vitro cell culture assays. Cells were starved for 4 h before the addition of growth factors. Concentrations used were the following: TGF-β, 10 ng/ml; BMP9, 50 ng/ml; VEGF-A, 20 ng/ml; RAP-041, 500 ng/ml; and SB431542 (Sigma–Aldrich), 5 μM. Stimulation proceeded for 48 h, after which cells were further processed for isolation of RNA (see the Quantitative RT-PCR section) or quantification of proliferation. Proliferation was assessed by immunostaining with Ki67 antibody (1:1,000 dilution; Leica). The proliferative index was expressed as percentage of positive cells and was assessed in 10–15 high-power fields per culture condition (in vitro) or mouse (in vivo).

Ex vivo angiogenic sprouting assay. RIP1-Tag2 mice were perfused with PBS and the pancreas of four mice were dissected and minced into small pieces. Angiogenic islets were isolated by collagenase (Sigma–Aldrich) digestion at 37°C for 12 min. Separation was achieved by Ficoll gradient centrifugation, and overtly angiogenic islets were picked by hand under a dissection microscope. Subsequently, the islets were incorporated in Matrigel basement membrane, which was growth factor reduced without Phenol Red (BD), containing a suspension of MS1 cells with the addition of 10 ng/ml TGF-β, 50 ng/ml BMP9, 1 μg/ml RAP-041, or combinations thereof, before the matrix was allowed to gel. Assessment of migration/sprouting of MS1 cells was performed by computer-aided quantification of the area covered by the MS1 cells surrounding the angiogenic islet in relation to the area covered by the angiogenic islet.

Statistical analysis. All measurements are depicted as mean ± SD. All analyses used the Student's double-sided unpaired t test, with P < 0.05 considered as statistically significant.

Online supplemental material. Fig. S1 presents expression of TGF-β family ligands and receptors in preparations from normal and neoplastic pancreas, as well as isolated cell lines. Fig. S2 presents expression of TGF-β receptors in ALK1-deficient and WT RIP1-Tag2 tumors. Fig. S3 demonstrates inhibition of bFGF-induced angiogenesis by RAP-041. Fig. S4 presents the lack of direct effect of RAP-041 on the proliferation and apoptosis of β TC3 cells. Fig. S5 presents the synergistic effects of combining TGF-β and BMP9 on VEGF-induced proliferation of three different endothelial cell lines. Fig. S6 presents the expression of ALK1 and ALK5 target genes during RIP1-Tag2 tumorigenesis. Fig. S7 presents the synergistic induction of ALK5 target genes by TGF-β and BMP9. Online supplemental material is available at http://www.jem.org/cgi/content/full/jem.20091309/DC1.

REFERENCES

Arbiser, J.L., M.A. Moses, C.A. Fernandez, N. Ghiso, Y. Cao, N. Klauber, D. Frank, M. Brownlee, E. Flynn, S. Parangi, et al. 1997. Oncogenic H-ras stimulates tumor angiogenesis by two distinct pathways. *Proc. Natl. Acad. Sci. USA.* 94:861–866. doi:10.1073/pnas.94.3.861

Arthur, H.M., J. Ure, A.J. Smith, G. Renforth, D.I. Wilson, E. Torsney, R. Charlton, D.V. Parums, T. Jowett, D.A. Marchuk, et al. 2000. Endoglin, an ancillary TGFβ receptor, is required for extraembryonic angiogenesis and plays a key role in heart development. *Dev. Biol.* 217:42–53. doi:10.1006/dbio.1999.9534

Bajou, K., H. Peng, W.E. Laug, C. Maillard, A. Noel, J.M. Foidart, J.A. Martial, and Y.A. DeClerck. 2008. Plasminogen activator inhibitor-1 protects endothelial cells from FasL-mediated apoptosis. *Cancer Cell.* 14:324–334. doi:10.1016/j.ccr.2008.08.012

Bergers, G., and D. Hanahan. 2008. Modes of resistance to anti-angiogenic therapy. *Nat. Rev. Cancer.* 8:592–603. doi:10.1038/nrc2442

Bergers, G., K. Javaherian, K.M. Lo, J. Folkman, and D. Hanahan. 1999. Effects of angiogenesis inhibitors on multistage carcinogenesis in mice. *Science.* 284:808–812. doi:10.1126/science.284.5415.808

Bergers, G., S. Song, N. Meyer-Morse, E. Bergsland, and D. Hanahan. 2003. Benefits of targeting both pericytes and endothelial cells in the tumor vasculature with kinase inhibitors. *J. Clin. Invest.* 111:1287–1295.

Buijs, J.T., C.A. Rentsch, G. van der Horst, P.G. van Overveld, A. Wetterwald, R. Schwaninger, N.V. Henriquez, P. Ten Dijke, F. Borovecki, R. Markwalder, et al. 2007. BMP7, a putative regulator of epithelial homeostasis in the human prostate, is a potent inhibitor of prostate cancer bone metastasis in vivo. *Am. J. Pathol.* 171:1047–1057. doi:10.2353/ajpath.2007.070168

David, L., C. Mallet, S. Mazerbourg, J.J. Feige, and S. Bailly. 2007. Identification of BMP9 and BMP10 as functional activators of the orphan activin receptor-like kinase 1 (ALK1) in endothelial cells. *Blood.* 109:1953–1961. doi:10.1182/blood-2006-07-034124

Deckers, M.M., R.L. van Bezooijen, G. van der Horst, J. Hoogendam, C. van Der Bent, S.E. Papapoulos, and C.W. Löwik. 2002. Bone morphogenetic proteins stimulate angiogenesis through osteoblast–derived vascular endothelial growth factor A. *Endocrinology.* 143:1545–1553. doi:10.1210/en.143.4.1545

Deng, G., S.A. Curriden, S. Wang, S. Rosenberg, and D.J. Loskutoff. 1996. Is plasminogen activator inhibitor–1 the molecular switch that governs urokinase receptor–mediated cell adhesion and release? *J. Cell Biol.* 134:1563–1571. doi:10.1083/jcb.134.6.1563

Dennler, S., S. Itoh, D. Vivien, P. ten Dijke, S. Huet, and J.M. Gauthier. 1998. Direct binding of Smad3 and Smad4 to critical TGF beta-inducible elements in the promoter of human plasminogen activator inhibitor-type 1 gene. *EMBO J.* 17:3091–3100. doi:10.1093/emboj/17.11.3091

Efrat, S., S. Linde, H. Kofod, D. Spector, M. Delannoy, S. Grant, D. Hanahan, and S. Baekkeskov. 1988. Beta-cell lines derived from transgenic mice expressing a hybrid insulin gene-oncogene. *Proc. Natl. Acad. Sci. USA.* 85:9037–9041. doi:10.1073/pnas.85.23.9037

Ellis, L.M., and D.J. Hicklin. 2008. VEGF-targeted therapy: mechanisms of anti-tumour activity. *Nat. Rev. Cancer.* 8:579–591. doi:10.1038/nrc2403

Escudier, B., T. Eisen, W.M. Stadler, C. Szczylik, S. Oudard, M. Siebels, S. Negrier, C. Chevreau, E. Solska, A.A. Desai, et al; TARGET Study Group. 2007. Sorafenib in advanced clear-cell renal-cell carcinoma. *N. Engl. J. Med.* 356:125–134. doi:10.1056/NEJMoa060655

Goumans, M.-J., G. Valdimarsdottir, S. Itoh, A. Rosendahl, P. Sideras, and P. ten Dijke. 2002. Balancing the activation state of the endothelium via two distinct TGF-β type I receptors. *EMBO J.* 21:1743–1753. doi:10.1093/emboj/21.7.1743

Goumans, M.J., F. Lebrin, and G. Valdimarsdottir. 2003a. Controlling the angiogenic switch: a balance between two distinct TGF-β receptor signaling pathways. *Trends Cardiovasc. Med.* 13:301–307. doi:10.1016/S1050-1738(03)00142-7

Goumans, M.J., G. Valdimarsdottir, S. Itoh, F. Lebrin, J. Larsson, C. Mummery, S. Karlsson, and P. ten Dijke. 2003b. Activin receptor-like

kinase (ALK)1 is an antagonistic mediator of lateral TGFβ/ALK5 signaling. *Mol. Cell.* 12:817–828. doi:10.1016/S1097-2765(03)00386-1

Goumans, M.J., Z. Liu, and P. ten Dijke. 2009. TGF-β signaling in vascular biology and dysfunction. *Cell Res.* 19:116–127. doi:10.1038/cr.2008.326

Hanahan, D. 1985. Heritable formation of pancreatic β-cell tumours in transgenic mice expressing recombinant insulin/simian virus 40 oncogenes. *Nature.* 315:115–122. doi:10.1038/315115a0

Hawinkels, L.J., K. Zuidwijk, H.W. Verspaget, E.S. de Jonge-Muller, W. van Duijn, V. Ferreira, R.D. Fontijn, G. David, D.W. Hommes, C.B. Lamers, and C.F. Sier. 2008. VEGF release by MMP-9 mediated heparan sulphate cleavage induces colorectal cancer angiogenesis. *Eur. J. Cancer.* 44:1904–1913. doi:10.1016/j.ejca.2008.06.031

Hurwitz, H., L. Fehrenbacher, W. Novotny, T. Cartwright, J. Hainsworth, W. Heim, J. Berlin, A. Baron, S. Griffing, E. Holmgren, et al. 2004. Bevacizumab plus irinotecan, fluorouracil, and leucovorin for metastatic colorectal cancer. *N. Engl. J. Med.* 350:2335–2342. doi:10.1056/NEJMoa032691

Inoue, M., J.H. Hager, N. Ferrara, H.P. Gerber, and D. Hanahan. 2002. VEGF-A has a critical, nonredundant role in angiogenic switching and pancreatic β cell carcinogenesis. *Cancer Cell.* 1:193–202. doi:10.1016/S1535-6108(02)00031-4

Korchynskyi, O., and P. ten Dijke. 2002. Identification and functional characterization of distinct critically important bone morphogenetic protein-specific response elements in the Id1 promoter. *J. Biol. Chem.* 277:4883–4891. doi:10.1074/jbc.M111023200

Kortlever, R.M., P.J. Higgins, and R. Bernards. 2006. Plasminogen activator inhibitor-1 is a critical downstream target of p53 in the induction of replicative senescence. *Nat. Cell Biol.* 8:877–884. doi:10.1038/ncb1448

Kortlever, R.M., J.H. Nijwening, and R. Bernards. 2008. Transforming growth factor-beta requires its target plasminogen activator inhibitor-1 for cytostatic activity. *J. Biol. Chem.* 283:24308–24313. doi:10.1074/jbc.M803341200

Lamouille, S., C. Mallet, J.J. Feige, and S. Bailly. 2002. Activin receptor-like kinase 1 is implicated in the maturation phase of angiogenesis. *Blood.* 100:4495–4501. doi:10.1182/blood.V100.13.4495

Lyden, D., A.Z. Young, D. Zagzag, W. Yan, W. Gerald, R. O'Reilly, B.L. Bader, R.O. Hynes, Y. Zhuang, K. Manova, and R. Benezra. 1999. Id1 and Id3 are required for neurogenesis, angiogenesis and vascularization of tumour xenografts. *Nature.* 401:670–677. doi:10.1038/44334

Motzer, R.J., T.E. Hutson, P. Tomczak, M.D. Michaelson, R.M. Bukowski, O. Rixe, S. Oudard, S. Negrier, C. Szczylik, S.T. Kim, et al. 2007. Sunitinib versus interferon α in metastatic renal-cell carcinoma. *N. Engl. J. Med.* 356:115–124. doi:10.1056/NEJMoa065044

Moustakas, A., and C.H. Heldin. 2005. Non-Smad TGF-beta signals. *J. Cell Sci.* 118:3573–3584. doi:10.1242/jcs.02554

Oh, S.P., T. Seki, K.A. Goss, T. Imamura, Y. Yi, P.K. Donahoe, L. Li, K. Miyazono, P. ten Dijke, S. Kim, and E. Li. 2000. Activin receptor-like kinase 1 modulates transforming growth factor-β 1 signaling in the regulation of angiogenesis. *Proc. Natl. Acad. Sci. USA.* 97:2626–2631. doi:10.1073/pnas.97.6.2626

Pàez-Ribes, M., E. Allen, J. Hudock, T. Takeda, H. Okuyama, F. Viñals, M. Inoue, G. Bergers, D. Hanahan, and O. Casanovas. 2009. Antiangiogenic therapy elicits malignant progression of tumors to increased local invasion and distant metastasis. *Cancer Cell.* 15:220–231. doi:10.1016/j.ccr.2009.01.027

Pardali, K., and A. Moustakas. 2007. Actions of TGF-β as tumor suppressor and pro-metastatic factor in human cancer. *Biochim. Biophys. Acta.* 1775:21–62.

Park, S.O., Y.J. Lee, T. Seki, K.H. Hong, N. Fliess, Z. Jiang, A. Park, X. Wu, V. Kaartinen, B.L. Roman, and S.P. Oh. 2008. ALK5- and TGFBR2-independent role of ALK1 in the pathogenesis of hereditary hemorrhagic telangiectasia type 2. *Blood.* 111:633–642. doi:10.1182/blood-2007-08-107359

Persson, U., H. Izumi, S. Souchelnytskyi, S. Itoh, S. Grimsby, U. Engström, C.H. Heldin, K. Funa, and P. ten Dijke. 1998. The L45 loop in type I receptors for TGF-β family members is a critical determinant in specifying Smad isoform activation. *FEBS Lett.* 434:83–87. doi:10.1016/S0014-5793(98)00954-5

Pertovaara, L., A. Kaipainen, T. Mustonen, A. Orpana, N. Ferrara, O. Saksela, and K. Alitalo. 1994. Vascular endothelial growth factor is induced in response to transforming growth factor-β in fibroblastic and epithelial cells. *J. Biol. Chem.* 269:6271–6274.

Piek, E., A. Moustakas, A. Kurisaki, C.-H. Heldin, and P. ten Dijke. 1999. TGF-β type I receptor/ALK-5 and Smad proteins mediate epithelial to mesenchymal transdifferentiation in NMuMG breast epithelial cells. *J. Cell Sci.* 112:4557–4568.

Pietras, K., and D. Hanahan. 2005. A multitargeted, metronomic, and maximum-tolerated dose "chemo-switch" regimen is antiangiogenic, producing objective responses and survival benefit in a mouse model of cancer. *J. Clin. Oncol.* 23:939–952. doi:10.1200/JCO.2005.07.093

Pietras, K., T. Sjöblom, K. Rubin, C.H. Heldin, and A. Ostman. 2003. PDGF receptors as cancer drug targets. *Cancer Cell.* 3:439–443. doi:10.1016/S1535-6108(03)00089-8

Pourgholami, M.H., and D.L. Morris. 2008. Inhibitors of vascular endothelial growth factor in cancer. *Cardiovasc. Hematol. Agents Med. Chem.* 6:343–347. doi:10.2174/187152508785909528

Ramoshebi, L.N., and U. Ripamonti. 2000. Osteogenic protein-1, a bone morphogenetic protein, induces angiogenesis in the chick chorioallantoic membrane and synergizes with basic fibroblast growth factor and transforming growth factor-beta1. *Anat. Rec.* 259:97–107. doi:10.1002/(SICI)1097-0185(20000501)259:1<97::AID-AR11>3.0.CO;2-O

Roelen, B.A., M.A. van Rooijen, and C.L. Mummery. 1997. Expression of ALK-1, a type 1 serine/threonine kinase receptor, coincides with sites of vasculogenesis and angiogenesis in early mouse development. *Dev. Dyn.* 209:418–430. doi:10.1002/(SICI)1097-0177(199708)209:4<418::AID-AJA9>3.0.CO;2-L

Rusnati, M., and M. Presta. 2007. Fibroblast growth factors/fibroblast growth factor receptors as targets for the development of anti-angiogenesis strategies. *Curr. Pharm. Des.* 13:2025–2044. doi:10.2174/138161207781039689

Sadick, H., M. Sadick, K. Götte, R. Naim, F. Riedel, G. Bran, and K. Hörmann. 2006. Hereditary hemorrhagic telangiectasia: an update on clinical manifestations and diagnostic measures. *Wien. Klin. Wochenschr.* 118:72–80. doi:10.1007/s00508-006-0561-x

Scharpfenecker, M., M. van Dinther, Z. Liu, R.L. van Bezooijen, Q. Zhao, L. Pukac, C.W. Löwik, and P. ten Dijke. 2007. BMP-9 signals via ALK1 and inhibits bFGF-induced endothelial cell proliferation and VEGF-stimulated angiogenesis. *J. Cell Sci.* 120:964–972. doi:10.1242/jcs.002949

Schmierer, B., and C.S. Hill. 2007. TGFβ-SMAD signal transduction: molecular specificity and functional flexibility. *Nat. Rev. Mol. Cell Biol.* 8:970–982. doi:10.1038/nrm2297

Seoane, J. 2008. The TGFBeta pathway as a therapeutic target in cancer. *Clin. Transl. Oncol.* 10:14–19. doi:10.1007/s12094-008-0148-2

Shi, Y., and J. Massagué. 2003. Mechanisms of TGF-β signaling from cell membrane to the nucleus. *Cell.* 113:685–700. doi:10.1016/S0092-8674(03)00432-X

Srinivasan, S., M.A. Hanes, T. Dickens, M.E. Porteous, S.P. Oh, L.P. Hale, and D.A. Marchuk. 2003. A mouse model for hereditary hemorrhagic telangiectasia (HHT) type 2. *Hum. Mol. Genet.* 12:473–482. doi:10.1093/hmg/ddg050

Suzuki, Y., K. Montagne, A. Nishihara, T. Watabe, and K. Miyazono. 2008. BMPs promote proliferation and migration of endothelial cells via stimulation of VEGF-A/VEGFR2 and angiopoietin-1/Tie2 signalling. *J. Biochem.* 143:199–206. doi:10.1093/jb/mvm215

ten Dijke, P., and H.M. Arthur. 2007. Extracellular control of TGFβ signalling in vascular development and disease. *Nat. Rev. Mol. Cell Biol.* 8:857–869. doi:10.1038/nrm2262

Torsney, E., R. Charlton, A.G. Diamond, J. Burn, J.V. Soames, and H.M. Arthur. 2003. Mouse model for hereditary hemorrhagic telangiectasia has a generalized vascular abnormality. *Circulation.* 107:1653–1657. doi:10.1161/01.CIR.0000058170.92267.00

Venetsanakos, E., A. Mirza, C. Fanton, S.R. Romanov, T. Tlsty, and M. McMahon. 2002. Induction of tubulogenesis in telomerase-immortalized human microvascular endothelial cells by glioblastoma cells. *Exp. Cell Res.* 273:21–33. doi:10.1006/excr.2001.5424

Wu, X., J. Ma, J.D. Han, N. Wang, and Y.G. Chen. 2006. Distinct regulation of gene expression in human endothelial cells by TGF-β and its receptors. *Microvasc. Res.* 71:12–19. doi:10.1016/j.mvr.2005.11.004